

COMPARISON OF MULTI-FIDELITY ROTOR ANALYSIS TOOLS FOR TRANSITIONAL AND LOW SPEED FLIGHT REGIMES

D. Perdolt*, M. Thiele*, D. Milz†, M. May†, R. Kuchar†, M. Hornung*

* Technical University of Munich, Institute of Aircraft Design, Boltzmannstr 15, 85748 Garching, Germany

† German Aerospace Center, Institute of System Dynamics and Control, Münchener Straße 20, 82234 Weßling, Germany

Abstract

Urban and regional air mobility is a new mode of transportation currently attracting a lot of attention. Much effort is being put into preliminary design studies for various electric vertical takeoff and landing (eVTOL) concepts. Especially the aerodynamic modeling poses major challenges to both applications, the preliminary design and the control design of eVTOLs. One main factor affecting aerodynamic complexity is rotor aerodynamics and the respective couplings with other rotors, wings, and airframe. Thus, both applications share the need for a fast and user-friendly, yet sufficiently accurate analysis tool. This study provides an overview of four different rotor aerodynamic tools suitable for the preliminary and control design task of eVTOLs and a respective tool-selection for different applications. A cross-method comparison is performed for the tools *DUST*, *FLOWLab*, *SARF* and *OpenVSP/VSPAero*, with a focus on capturing complex rotor, rotor-rotor and rotor-wing aerodynamics. The Caradonna-Tung rotor, for which experimental data is available, represents the benchmark case. Subsequently, the Airbus A³ Vahana is used to extend the analysis to an aerodynamically complex eVTOL configuration for which a main wing rotor is analyzed. There, the rotor aerodynamics is analyzed in different flight phases, i.e., different phases of the transition. The comparison of the two cases shows possibilities and limitations with respect to the quality of the computational results and handling aspects of the respective tools. The results suggest that *DUST* provides accurate results and covers most relevant effects at the cost of higher computational complexity. Both, the *FLOWLab* tools as well as *SARF* provide sufficiently accurate results in a short time. Though, *SARF* does not cover friction drag and thus underestimates the rotor torque. *OpenVSP* often shows convergence issues, but otherwise shows comparable results to the previous two tools.

Keywords

Rotor Analysis; eVTOL; Urban Air Mobility; Vahana, *DUST*, *FLOWLab*, *SARF*, *OpenVSP*, *VSPAero*

1. INTRODUCTION

Today's battery and electric propulsion technologies are facilitating the development of urban air mobility (UAM) and regional air mobility (RAM), which are new and increasingly important mobility concepts with the potential to reduce travel times and change travel patterns [1, 2, 3]. Most UAM and RAM concepts are likely to be realized by aircraft that are configured to take off and land vertically and are also equipped with electric motors for propulsion (eVTOLs) [4]. These vehicles promise the flexibility of helicopters during take-off and landing and the efficient forward flight of aircraft at the cost of a complex control task [5].

Although many companies are working on such eVTOL concepts, important aspects of these concepts still need to be analyzed and understood [1]. The design of these vehicles poses great challenges due to vastly extended design space, limited availability of empirical data and complex aerodynamics with respect to diverse interactions [6, 7, 8, 9]. During the preliminary design phase, a large number of configurative studies and simulations are performed. Beyond that, the development of eVTOL control architectures requires a sufficiently accurate, yet per-

formant aerodynamic model of the aircraft [10, 11, 12]. Thus, the demand for tools that are capable to cover the interactions between rotors, wings, airframe and ground while allowing a fast and reliable analysis with minimal manual geometric pre-processing is high [13].

This paper presents a comparison of selected, existing and actively maintained tools, that are suitable for aerodynamic rotor analyses and model creation suitable for the preliminary and control design task of eVTOLs. Suitability is determined based on predefined criteria. The tools should be able to capture relevant interactions like rotor-wing and rotor-rotor interactions and should provide evaluation possibilities that can be used for comparison. They should already be used for VTOL configurations and, if possible, be open source. The prospect of a quick, easy and user-friendly implementation of a model for design and control is of great importance in the selection. *DUST* developed by Airbus A³ and the Politecnico di Milano, the package of tools developed by *FLOWLab*, *SARF* from TU Munich, and *OpenVSP*, which includes *VSPAero*, are considered. The tools discussed have been validated against experimental or CFD data by the respective developers. Nevertheless, no detailed compar-

ison between the tools with respect to VTOLs has yet been carried out.

In a first step, the Caradonna-Tung rotor benchmark case [14] is evaluated in order to assess the individual tool's abilities to capture „classical“ rotor aerodynamic phenomena. It is implemented in all tools, correlated with reference data and compared across the methods to quantify discrepancies in the tool's numeric models.

In a second step, the capabilities of the tools are then tested on an eVTOL aircraft configuration, the A³ Vahana. A focus is set on complex aerodynamically complex interactions exhibited on a main wing rotor during the VTOL transition flight state. Therefore, the aerodynamics of this rotor is analyzed for the different flight states.

The analysis of the benchmark case and the VTOL transition case shows the possibilities of the individual tools and the accuracy of converged data. The chosen analyses should also highlight possible limitations in the models. In addition, subjective handling criteria for end-users will be discussed. The most promising tools will be used to simulate the aerodynamics required for the development of eVTOL control architectures in future work.

Although the seemingly most suitable tools have been selected, there are other promising approaches for the analysis of eVTOL aerodynamics. Those include *NDARC* [15, 16], the CFD tool *AcuSuolve* [17], *HPCMP CREATETM-AV* [18], or a strip theory approach as shown in [19].

2. ROTOR ANALYSIS TOOLS

The rotor aerodynamics tools used in this work rely on different numerical methods. Each tool features an individual approach to the assessment of VTOL configurations, which makes a direct comparison challenging while at the same time offers the opportunity to select a fitting tool for different tasks.

2.1. DUST

The first of the four considered tools is *DUST*, a medium-fidelity aerodynamic open source software. *DUST* is the result of a collaboration between Politecnico di Milano and A³ by Airbus and was developed to provide a fast, accurate and flexible tool for the aerodynamic analysis of rotorcraft and eVTOLs [20]. It is designed to enable aerodynamic simulations of complex aircraft configurations by representing interactive aerodynamic interactions and phenomena in a reliable and, above all, robust manner [20]. *DUST* can be used for aerodynamic analysis of conventional aircraft, helicopters and eVTOLs and any other vehicle configuration flying under any flight conditions [20]. *DUST* is described and validated in [20, 21]. The solution implemented in *DUST* relies on the Helmholtz decomposition of the velocity field to recast the aerodynamic problem as a mixed boundary elements-vortex particles method (VPM [22, 23]) [20]. Different aerodynamic elements can be combined in a single model to accurately capture the relevant physical phenomena, while an accelerated vortex particle model of the wake area allows for a numerically stable La-

grangian description of the free vorticity evolution [21]. The aerodynamic elements include lifting lines (LL), vortex-lattice method (VLM) and surface panels (SP). Pressure field evaluation in a rotational flow relies on an integral boundary problem for the Bernoulli polynomial obtained from the Navier–Stokes equation [21]. *DUST* has been validated against numerical and experimental data available for conventional vehicle configurations as well as architectures with complex interactions, such as a rotor-tilt-wing system in hover and forward flight [20, 21].

2.2. FLOWLab

The *FLOWLab* research laboratory at Brigham Young University in Utah develops various aerodynamic tools for aircraft design [24]. One of these aerodynamic tools is called „*FLOWUnsteady*“, described in [25, 26, 27, 28, 29]. *FLOWUnsteady* is a simulation tool for mixed-fidelity transient aerodynamics and aeroacoustics. The tool combines the following medium and high fidelity aerodynamics tools developed at BYU's *FLOWLab*: *GeometricTools* („geometric engine“), *FLOWVLM* („VLM and strip theory solver“), *CCBlade* („blade element momentum solver“), *MyPanel* („3D inviscid panel solver“) and *FLOWVPM* („viscous vortex particle method“) [24]. *FLOWUnsteady* was developed primarily with the aim of analyzing eVTOL configurations during the transition phase [28].

The VPM solver, which is described and evaluated in [25, 29], used in *FLOWUnsteady* is not publicly available. Instead, the quasi-steady solver, evaluated in [28], is available for open source use. It captures wing-rotor interactions acceptably, while, according to *FLOWLab* [28], rotor-rotor interactions are only minimally considered.

2.3. SARF

SARF (Synthesis and Analysis of Rotor Framework) is a propeller design environment implemented at TU Munich in MATLAB for the calculation and analysis of rotors [30]. The validated, flexible and extensible framework enables the analysis of rotor performance and wake interactions with other elements of an aircraft [30]. Conducting the analysis with this tool is relatively simple and fast and can be performed with sufficient accuracy for many applications. It can be used for a wide range of rotor configurations and flow states [31]. It is furthermore possible to apply a rotor synthesis algorithm for given operating points [30]. Use cases for the tool are the creation of configuration studies assessing the optimal placement of propellers on a UAV or the calculation of rotor characteristics during a flight mission as an input to other applications, such as the development of a controller to avoid vibrations [30, 31].

The integrated doublet-lattice method (DLM) enables the wake geometry of rotors to be calculated for any transient boundary condition according to the potential theory [31]. It is also possible to model the wake of other aerodynamically acting objects with their wake and the mutual wake interactions through the adaption and consideration of various additional numerical effects, as de-

scribed in [31]. The application of these effects on all objects greatly improves the vortex behavior near obstacles while the vortex separation algorithm enables realistic interaction simulation of the vortex sheets with an obstacle beyond the scope of the classical potential theory considerations [31].

This enables the investigation of interaction effects between the rotor, obstacles and other wake elements. In addition, the developed rotor wake simulation offers the possibility to assess the development of new propulsion concepts for UAVs [31]. The results of the methodology have been validated extensively with experimental data and simulation results in [31], showing good agreement. *SARF* is not yet open source available for the time being.

2.4. OpenVSP/VSPAero

OpenVSP (Vehicle Sketch Pad) is a geometry modeling tool developed by NASA for conceptual aircraft design, released in 2012 under the NASA Open Source Agreement [32, 33]. The software models conventional aircraft configurations with pre-configured basic geometric shapes and, unlike conventional CAD software, no prior knowledge is required for successful analysis [32].

OpenVSP allows the user to easily create a 3D model of an aircraft using general technical parameters, which can then be saved and exported in various formats for further analysis in other programs, mainly CFD [34]. However, *OpenVSP* also features the capabilities to directly analyze the 3D models. One of the tools integrated into the *OpenVSP* software is the analysis module *VSPAero* [35]. *VSPAero* is a thin-surface aerodynamic analysis program which is described in [36, 37]. It is a solver that includes both the vortex lattice method and the full panel method based on generalized vortex loops [37]. The core *VSPAero* solver is based on an agglomerated multi-pole approach, coupled with a preconditioned linear solver, to reduce solution times [37]. Adaptive wakes, time-accurate, unsteady analyses and propeller modeling are all supported [37].

3. APPLICATION

The configurations of the benchmark case and the VTOL transition case are modeled, simulated and analyzed. The calculation parameters have been adapted to the application and the tools' specifics while ensuring overall compatibility in terms of geometric and numerical discretization. Compatibility of the generated data was the first priority of the problem implementation. The data obtained was visualized and used to evaluate the aerodynamic parameters. Knowledge gained in the assessment of the benchmark calculations has been incorporated for the application of the VTOL transition case.

3.1. Means of Comparison

The calculations of the characteristic values, which are obtained during the application and compared in the discussion, are carried out either automatically by the tools or manually in post-processing.

The local lift coefficient C_l is calculated using (1). The total lift coefficient C_L (2) is then obtained by integrating the local lift coefficient C_l over the panels of the rotor.

$$(1) \quad C_l = \frac{2 \cdot dL}{\rho \cdot V_r^2 \cdot c \cdot dr}$$

$$(2) \quad C_L = \int_0^R C_l dr$$

The thrust coefficient C_T was calculated according to (3) with the thrust T . Similarly, the torque coefficient C_Q was calculated with the torque Q or with the moment about the rotor axis with (4).

$$(3) \quad C_T = \frac{T}{\rho \cdot n^2 \cdot D^4}$$

$$(4) \quad C_Q = \frac{Q}{\rho \cdot n^2 \cdot D^5}$$

For the Figure of Merit FOM , the modified form of the momentum theory with the non-ideal approximation for the power described by Leishman in [38] is used. For this modified theory, it is assumed that $C_{d_0} = 0.01$ and the induced power factor $\kappa = 1.15$, since non-ideal losses are assumed. σ denotes the rotor solidity and is calculated according to (6).

$$(5) \quad FOM = \frac{C_T^{3/2}}{\sqrt{2} \cdot C_P} = \frac{\frac{C_T^{3/2}}{\sqrt{2}}}{\frac{\kappa C_T^{3/2}}{\sqrt{2}} + \frac{\sigma C_{d_0}}{8}}$$

$$(6) \quad \sigma = \frac{N_b \cdot c}{\pi \cdot R}$$

The efficiency η is calculated following (7) with the advance ratio calculated according to (8).

$$(7) \quad \eta = \frac{C_T \cdot J}{2\pi \cdot C_Q}$$

$$(8) \quad J = \frac{V_{inf}}{n \cdot D}$$

3.2. Benchmark Case

For the benchmark case, the Caradonna-Tung rotor described in [14] and shown in fig. 1 is modeled by each of the tools and subsequently analyzed.

In order to cover the extensive experimental data well, a rotor speed in the low (1250 RPM), medium (1750 RPM) and higher speed range (2300 RPM) are chosen respectively. Simulations are performed for all rotor pitch angles (2° , 5° , 8° , 12°) for all selected rotor speeds.

3.2.1. DUST

The first tool to be considered is *DUST*. The simulation is set up and the rotor pitch angle varied for the different rotational speeds. The following simulation parameters are used to achieve stable results:

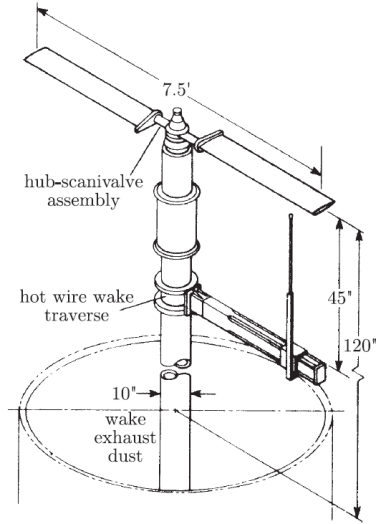


FIG 1. Experimental set-up of the Caradonna-Tung rotor [14]

- 15 revolutions per simulation
- 360 time steps per simulation
- Simulation duration = $\frac{\text{number of revolutions}}{\Omega_{Rotor}/60}$
- Time step = $\frac{\text{simulation duration}}{\text{number of time steps}}$
- „Vortex“ radius = 0.3 m
- „Rankine“ radius = 0.1 m

The Caradonna-Tung rotor analysis is shown in fig. 2. The wake is represented with particles due to the VPM. The vorticity of these particles is shown to indicate one of the possible representations of the variables, which is commonly used.

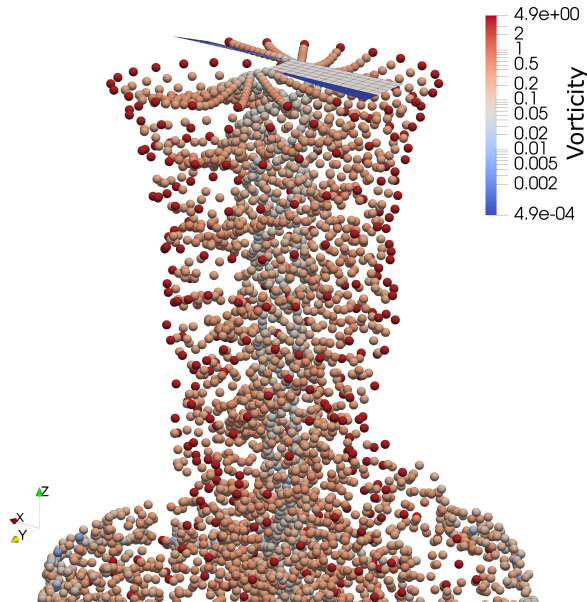


FIG 2. DUST - Implementation of the Caradonna-Tung rotor as a benchmark case

The simulation with the highest rotor speed $\Omega_{Rotor} = 2300$ RPM and the largest rotor pitch angle $\Theta_C = 12^\circ$ is illustrated. Thus, the state with the most pronounced wake is shown.

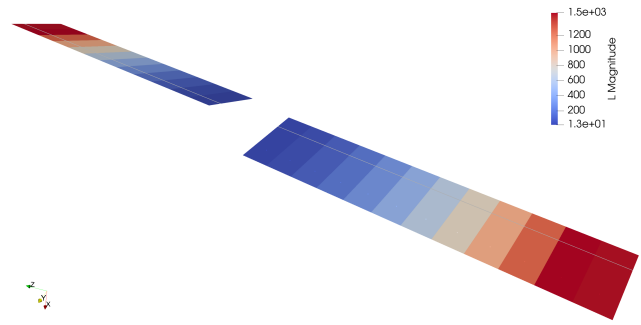


FIG 3. FLOWLab - Implementation of the Caradonna-Tung rotor as a benchmark case

3.2.2. FLOWLab

Next, the benchmark is analyzed with the aerodynamics tools developed by *FLOWLab*. As noted the VPM solver is not publicly available within the *FLOWUnsteady* package and therefore the quasi-steady solver with its VLM was used. The following settings were selected for the analysis of the geometry shown in fig. 1:

- 15 revolutions per simulation
- 360 time steps per simulation
- Simulation duration = $\frac{\text{number of revolutions}}{\Omega_{Rotor}/60}$
- Time step = $\frac{\text{simulation duration}}{\text{number of time steps}}$

The settings were chosen based on settings used in the examples provided by *FLOWLab*.

The visualization of the the simulation with the highest rotor speed $\Omega_{Rotor} = 2300$ RPM and the largest rotor pitch angle $\Theta_C = 12^\circ$ is shown in fig. 3. The figure shows the sectional lift that is produced by the rotor blades.

In this case, the wake is not visualized, but only the VLM panels on the lifting surfaces are indicated.

3.2.3. SARF

The Caradonna-Tung rotor is then modeled in *SARF* for all mentioned rotor pitch angles and all three rotational speeds. The simulation parameters are adapted to the application and the special features of *SARF*, in order to obtain a stable convergence. The main focus in the choice of simulation parameters is on the CFL (Courant-Friedrichs-Lewy) number, which is used to determine the appropriate time step length for the simulation:

$$(9) \quad \Delta t = CFL \frac{L_c}{U_c}$$

The time step length Δt is dependent on the CFL number and the characteristic cell length L_c , which is calculated from the discretization size and the characteristic flow velocity U_c , which is derived from the inflow velocity and the rotor speed.

The simulation parameters have been chosen as follows:

- 2.5 revolutions per simulation
- 200 time steps
- 120 trailing vortex elements

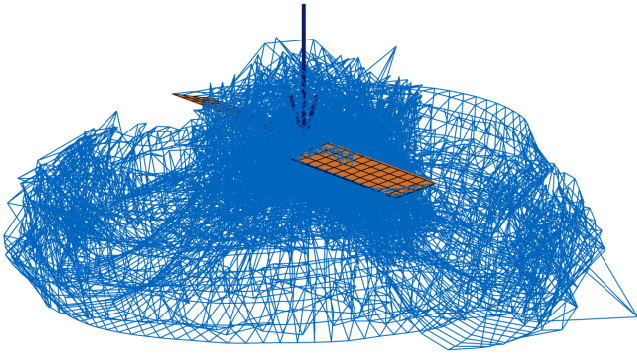


FIG 4. SARF - Implementation of the Caradonna-Tung rotor as a benchmark case

- CFL number = 2

The visualization of the simulation during the last time step with a rotor speed of $\Omega_{Rotor} = 2300$ RPM and a rotor pitch angle of $\Theta_C = 12^\circ$ is shown in fig. 4. The location of the individual vortices in the produced three-dimensional wake vortex sheets are shown in blue. The center of the rotor shows the vortices propagating in front of the rotor due to the induced downwash velocity being slightly underestimated for static thrust calculations.

3.2.4. OpenVSP/VSPAero

The simulations were set up in *OpenVSP/VSPAero* for the same flow states with the following settings:

- 15 revolutions
- 360 time steps
- Simulation time = $\frac{\text{number of revolutions}}{\Omega_{Rotor}/60}$
- Time step = $\frac{\text{simulation duration}}{\text{number of time steps}}$

The Caradonna-Tung rotor analysis with $\Omega_{Rotor} = 2300$ RPM and $\Theta_C = 12^\circ$ is shown in fig. 6.

The ΔC_p distribution on the rotor blades is shown as an example for the visualization of parameters. Beyond that, the vorticity, the steady pressure, the unsteady pressure as well as total pressure can be displayed. The wake vortex sheet geometry is shown in gray.

3.3. VTOL Transition Case

For the VTOL transition case, the Vahana with its tilt-wing system developed by A³ by Airbus was used. The demonstrator is shown in fig. 5.



FIG 5. Demonstrator of the A³ Vahana [39]

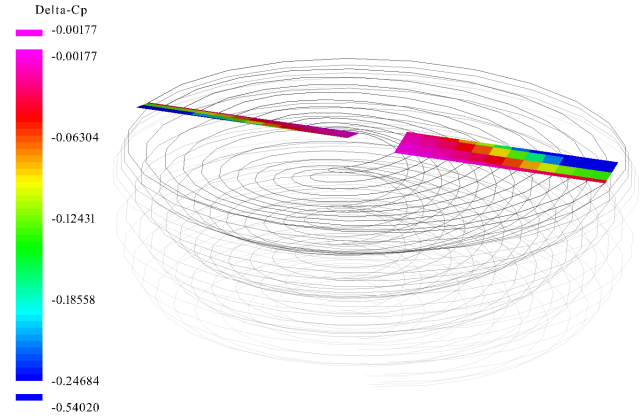


FIG 6. OpenVSP/VSPAero - Implementation of the Caradonna-Tung rotor as a benchmark case

The implementation of the VTOL Transition case is based on a work done by Politecnico di Milano and A³ by Airbus. In [20] a comprehensive analysis of the Vahana configuration has already been carried out by the developers of *DUST* and the developers of the Vahana. A comparison of test flight, CFD simulations and simulations in *DUST* for the Vahana configuration were performed. In addition to the analysis and validation of Vahana in *DUST*, trimmed flight conditions can be derived from the work, which are independently modeled and analyzed in *FLOWLab*, *SARF* and *OpenVSP/VSPAero*.

Several trimmed flight conditions were modeled in [20]: hover, climb and vertical descent in the „helicopter-mode“. In addition, two different forward flight conditions with 21 m s^{-1} and 36.3 m s^{-1} respectively were simulated during the transition from hover to cruise flight. For these simulated flight conditions, the configuration parameters measured in the associated flight tests were modeled. These settings include the rotor pitch angle Θ_C , the tilt angle of the canard and main wing, the angle of attack of the VTOL itself and the rotor speed Ω_{Rotor} . Except for information on the wing tilt angles, however, details on the configuration settings are not explicitly publicly available.

The rotor pitch angles were estimated because they are not explicitly mentioned in the work of A³ and Politecnico di Milano [20] used for Vahana. However, since [20] is preceded by an analysis of a single rotor, it can be assumed that these are analogous settings to the rotors for the whole Vahana configuration. Figure 7 shows how the associated rotor pitch angles Θ were estimated from the known tilt angles $\tau = 90^\circ, 60^\circ, 18.4^\circ$. The estimated rotor pitch angles Θ_C are shown in table 1.

For simplicity, a rotor speed of 3500 RPM, which was not known before, was chosen for all rotors based on commonly used rotor speeds of the MAGicALL motors used. The unknown incidence angles of the main and canard wing were chosen according to a Vahana geometry example provided by *FLOWLab* [40]. The incidence angle on the main wing corresponds to 7.5° and the incidence angle on the canard wing to 4° . NACA-0012 airfoils were used for the main and the canard wing. The APC10x7

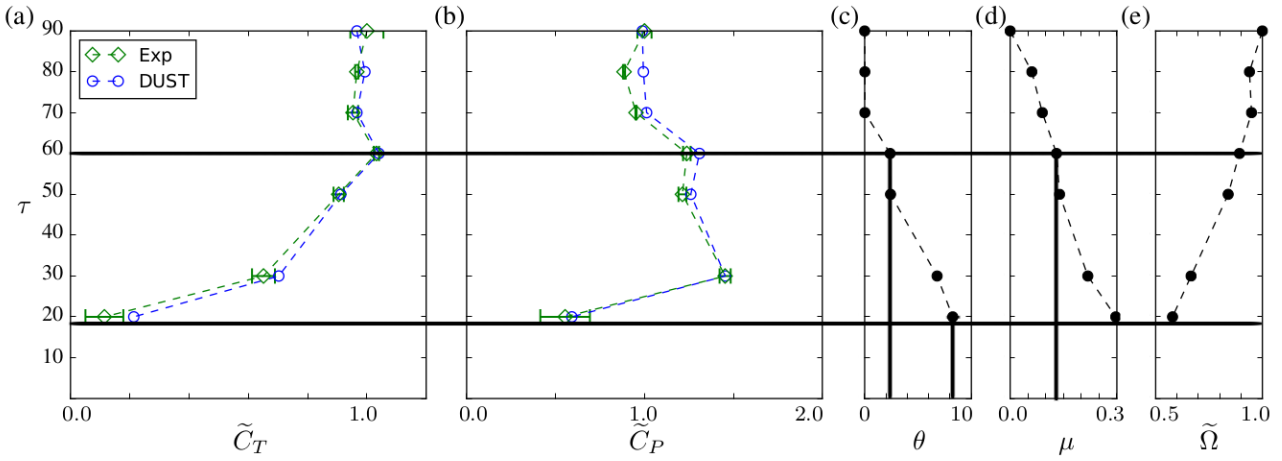


FIG 7. Determination of the rotor pitch angles Θ_C for the discussed flight conditions (Figure adapted from fig. 2. in [20])

propeller with three rotor blades was chosen for the rotor blades.

An overview of the flight states derived from [20] and the associated settings is given, which is subsequently modeled in *FLOWLab*, *SARF* and *OpenVSP/VSPAero*.

TAB 1. Discussed flight conditions for the VTOL transition case

Flight condition	V_{TAS} ($m s^{-1}$)	Ω_{Rotor} (RPM)	tilt angle ($^{\circ}$)	Θ_C ($^{\circ}$)
Climb	2.54	3500	90	0
Mid-transition	21	3500	60	2
Late-transition	36.3	3500	18.4	8

3.3.1. FLOWLab

The trimmed flight conditions, described in table 1 were then implemented using the tools of *FLOWLab*. The geometry itself could be obtained from a openly accessible example from *FLOWLab* [40]. The following simulation parameters were chosen:

- 200 time steps
- simulation time = 1.0 s
- time step = 0.005 s

Figure 8 shows the visualization of the flight condition in mid-transition analyzed with the *FLOWLab* tools package.

The circulation Γ is visualized on the wings and rotors. On closer inspection, the VLM used in the quasi-steady solver, which uses Γ to calculate the lift L , can again be seen on the wings. The climb and the late transition were simulated analogously.

3.3.2. SARF

Since *SARF* can only analyze one rotor/wing combination at a time, a wing section from the main wing of the Vahana with the associated rotor was chosen and modeled to evaluate the VTOL transition case. The rotor-

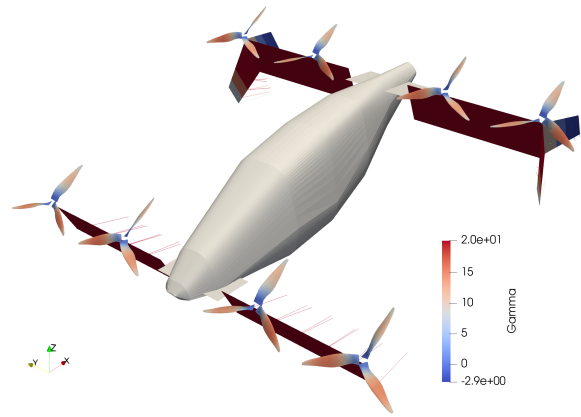


FIG 8. *FLOWLab* - Vahana full-vehicle analysis in mid-transition

wing combination was implemented for the flight conditions described in table 1. The following parameters were chosen to perform a stable calculation:

- 1.1 revolutions per simulation
- 90 time steps
- 80 wake vortex elements
- CFL number = 1.8

The analysis of the rotor/wing combination for the late-transition flight condition is shown in fig. 9 since the mid-transition flight condition has already been shown for *FLOWLab*.

3.3.3. OpenVSP/VSPAero

The flight states of the climb, mid-transition and late-transition were finally analyzed in *OpenVSP/VSPAero*. The geometry of the Vahana was created in *OpenVSP* and then analyzed in *VSPAero* using the VLM. The following parameters were set in *VSPAero*:

- 128 time steps
- 128 wake vortex elements
- 7 revolutions
- Simulation time = 0.128 s
- Time step = 0.001 s

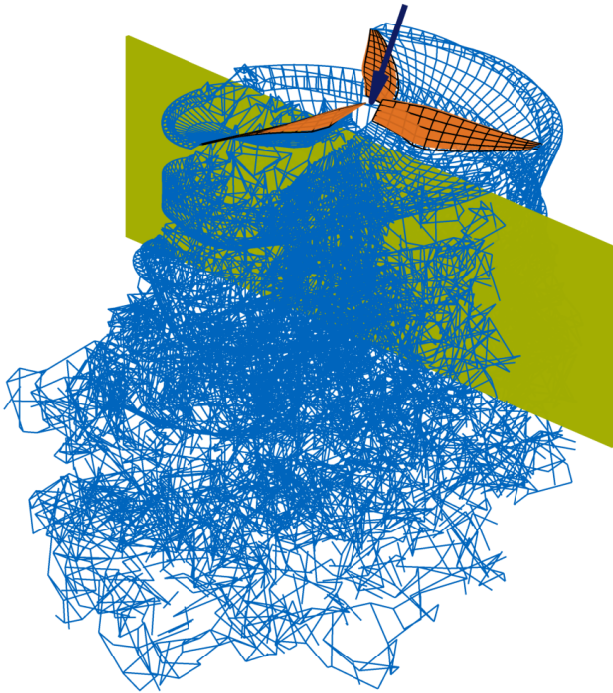


FIG 9. *SARF* - Simulation of a rotor/wing combination representing part of the Vahana wing in late-transition

Figure 10 shows the visualization of the last flight state, the late transition.

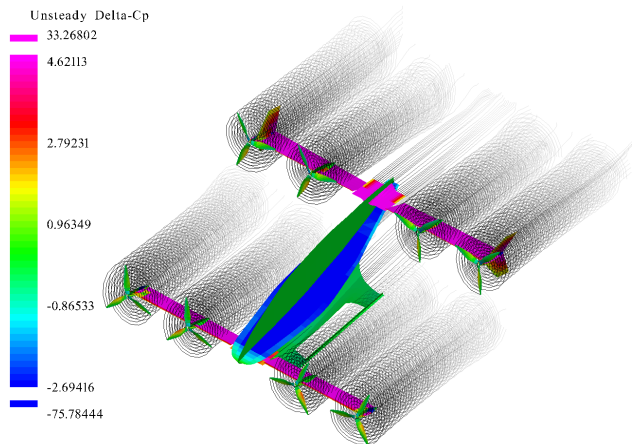


FIG 10. *OpenVSP/VSPAero* - Vahana full-vehicle analysis in late-transition

4. DISCUSSION

The results obtained for the benchmark case and the VTOL transition case are compared across methods. By comparing the characteristic values as well as the aspects of handling and use, the possibilities and limitations of the individual tools are derived.

4.1. Benchmark Case

The pressure distribution of the rotor was measured by Caradonna and Tung [14] at five radial sections ($r/R = 0.50, 0.68, 0.80, 0.89, 0.96$). From this, the lift coefficient

C_l for these sections was calculated and is now used to validate the individual tools. A representative combination of rotor speed Ω_{Rotor} and rotor pitch angle Θ_C was chosen from the measurement flow states.

Figure 11 compares the curves of the lift coefficient C_l for the range of $r/R = 0.5 - 0.96$ for a rotor speed of $\Omega_{Rotor} = 1250$ RPM with a rotor pitch angle of $\Theta_C = 8^\circ$.

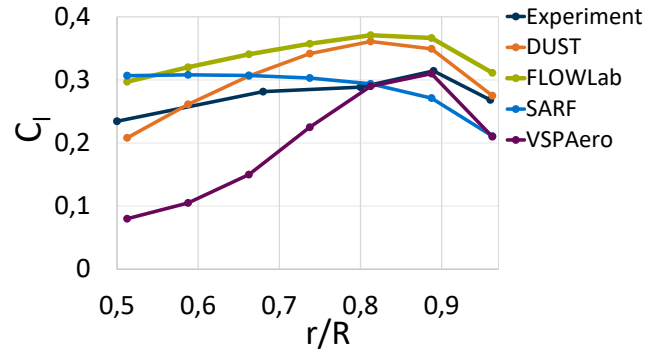


FIG 11. benchmark case: validation - distribution of the lift coefficient C_l

Despite deviations of the distributions of the lift coefficient C_l obtained in the tools, a good agreement with the experimental data can be seen in *DUST*, *FLOWLab* and *SARF*. For *VSPAero*, larger deviations can be identified towards the rotor center. However, towards the rotor tip, it is comparable to the other tools.

Further results of the tools validated with the experimental data are compared in the following figures. However, the evaluated characteristic values exceed the lift coefficient C_l analyzed in the validation. In the following, the experimental data of Cardonna and Tung [14] are not included, as they do not go beyond the radial distribution of the local lift coefficients.

Figure 12 compares the C_T values obtained in the four tools for 12 selected Θ_C/Ω_{Rotor} combinations.

Especially in the lower pitch angle range, for $\Theta_C = 2^\circ$ and 5° , the C_T values obtained for *DUST*, *FLOWLab* and *SARF* agree. In *OpenVSP/VSPAero*, the simulations performed for the rotor pitch angle of 2° were unstable, which meant that no meaningful data could be evaluated for this rotor pitch angle. Nevertheless, the C_T values for the next larger rotor pitch angle of 5° are comparable to the values obtained in the other tools. For the rotor pitch angle of 8° and 12° there is still comparability between *DUST* and *SARF*. The remaining two tools diverge more and more, resulting in larger values for C_T .

As can be seen in fig. 2, for example, a very pronounced wake develops at high rotor speeds Ω_{Rotor} and rotor pitch angles Θ_C . Due to different modeling of the wake in the tools, deviations are therefore to be expected. For the analysis with the *FLOWLab* tools, only the quasi-steady solver, using VLM, described in section 2.2 could be used. Similarly, no transient effects were considered with the VLM solver used in *VSPAero*. In both *SARF* and *DUST*, transient effects are taken into account. In *SARF* this is realized via DLM and in *DUST* the wake is modeled via an accelerated VPM. Since an increasingly unsteady behavior is to be expected with

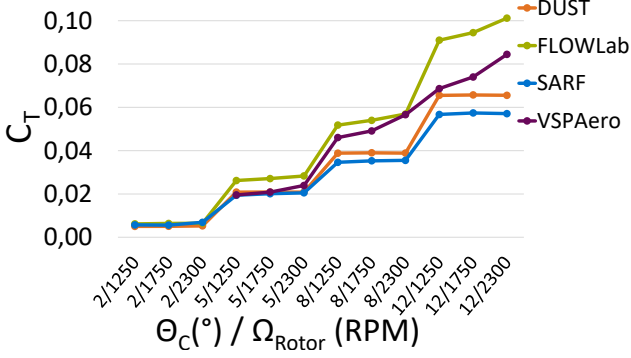


FIG 12. benchmark case: C_T comparison

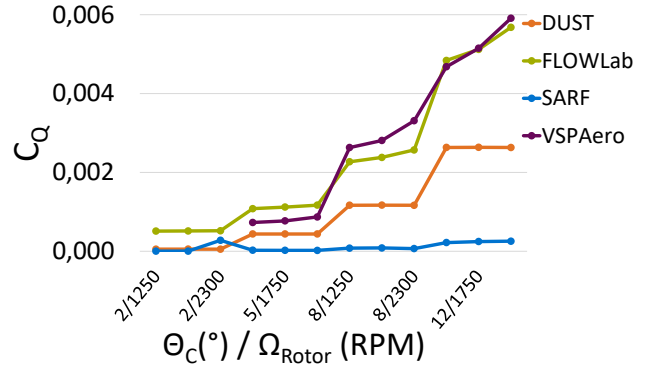


FIG 13. benchmark case: C_Q comparison

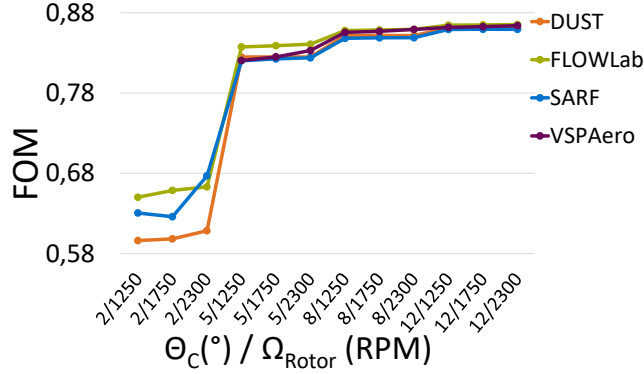


FIG 14. benchmark case: FOM comparison

increasing speed Ω_{Rotor} and larger rotor pitch angles Θ_C , it can be concluded that *DUST* and *SARF*, which map the unsteady effects, provide significantly more accurate results here. Whereas the calculations of *FLOWLab* and *VSPAero* deviate with increasing transient behavior. For *FLOWLab*, a better representation of the wake would be expected with the non-publicly available VPM solver, but also a longer computation time.

According to (3) one would expect that due to the nondimensionalization the values of the thrust coefficient C_T are independent of the rotor speed. While this is the case for *DUST* and *SARF*, for *OpenVSP/VSPAero* and *FLOWLab* $\Theta_C = 8^\circ$ and 12° result in larger C_T values with increasing Ω_{Rotor} .

The torque coefficient C_Q was compared analogously to C_T and shown in fig. 13. The C_Q curve for *DUST*, *FLOWLab* and *OpenVSP/VSPAero* shows a comparable characteristic to the discussed curve of the C_T values. The C_Q values of *DUST* are consistently below the values of *FLOWLab* and *OpenVSP/VSPAero*. This behavior could already be observed with the C_T value and could be due to the fact that neither *FLOWLab* nor *OpenVSP/VSPAero* capture transient effects. For *SARF*, however, it can be seen that the C_Q values are far below those of the other tools. This behavior results from the fact that no thickness effects are represented and therefore only the induced drag and thus the induced torque is considered. This is a clear shortcoming of *SARF* compared to the other tools.

To evaluate the rotor efficiency in hover flight, the Figure of Merit FOM was calculated in all four tools. The FOM describes the ratio between the ideal power required for hovering and the actual power required [38]. The results of the FOM calculated in the four tools are compared in fig. 14.

The comparison shown in fig. 12 has already indicated that C_T increases with increasing rotor pitch angle Θ_C . According to [38], the FOM converges towards $\frac{1}{\kappa} = 0.87$ with increasing C_T . All four tools show this characteristic with increasing rotor pitch angle Θ_C and thus increasing C_T and approach $\frac{1}{\kappa}$. At the low rotor pitch angle $\Theta_C = 2^\circ$ a deviation can be observed, which is however below 10%. As already mentioned, no stable results could be obtained in *VSPAero* for $\Theta_C = 2^\circ$. Nevertheless, the comparison of the FOM shows a good agreement between the tools.

4.2. VTOL Transition Case

The Vahana was successfully implemented in *DUST* by Politecnico di Milano and Airbus A³ [20]. The choice of modeling the components individually (SP, VLM, LL) allows a flexible setting of the fidelity [20]. It should be mentioned that especially the usage of surface panels (SP) enables the generation of an accurate model for streamlined bodies at small angles of attack [20]. However, these surface panels fail to represent flow separations and stalls because they overestimate the lift and underestimate the drag of the body [20]. Comparison with test values and CFD simulations have thus shown that *DUST* is capable of simulating a complex VTOL

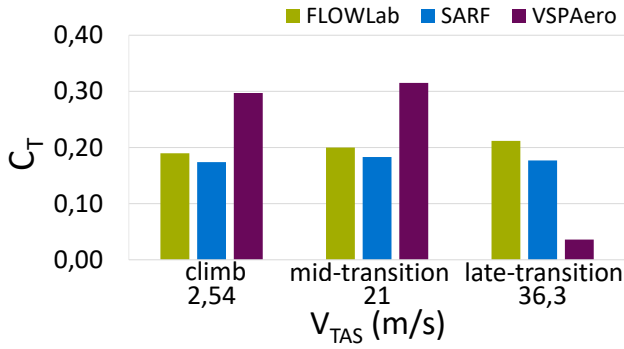


FIG 15. benchmark case: C_T comparison

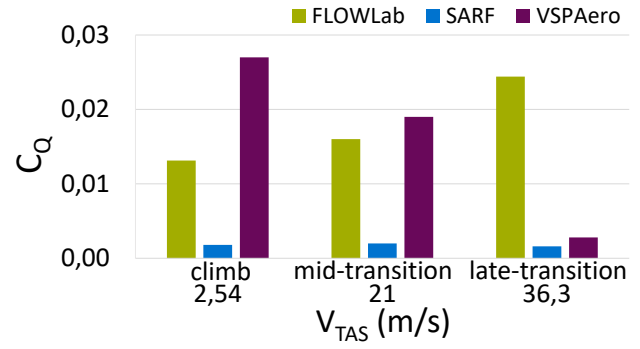


FIG 16. VTOL transition case: C_Q comparison

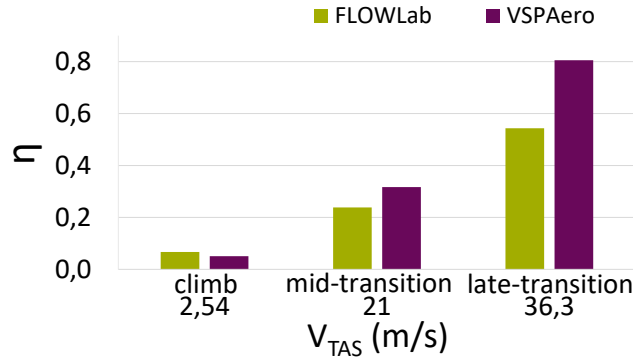


FIG 17. VTOL transition case: η comparison

configuration such as Vahana, provided there are no significant flow separations [20].

Three flight states of the transition flight were derived from the execution of the VTOL transition case in *DUST*. Figures 15 to 17 compare the characteristic values of the rotors for *FLOWLab*, *SARF* and *OpenVSP/VSPAero* obtained or calculated for the three flight conditions.

Over the three flight states of the transition flight C_T (fig. 15), C_Q (fig. 16) and the rotor efficiency η (fig. 17) are compared. For C_T , comparable values are obtained in *SARF* and *FLOWLab*. In *SARF*, C_T remains approximately constant. In *FLOWLab*, however, larger C_T values are obtained with the Θ_c increasing over the flight conditions. The efficiency η is not shown for *SARF* because the calculated C_Q values only consist of the induced torque.

Due to the rotation, the local incident flow of the rotor blades changes cyclically. This results in a strong transient variation of the aerodynamic forces, even during a stationary forward flight [41]. The unsteady variation of the aerodynamic forces on the rotor blades leads to vortex shedding as well as trailed vortices, which flow into the rotor wake [41]. In addition, the transient wake of a single rotor is influenced by other rotors and lifting surfaces. Since the tools use different modeling approaches to describe the flow of the wake, there are major deviations depending on the flight condition of the Vahana. The comparison shows hardly any similarities. Rather, the major differences in the modeling and approach of the calculation methodology become clear.

4.3. Advantages, Disadvantages and Tool-Usage

The model generation, simulation execution and post-processing of the benchmark case and the VTOL transition case and the cross-method comparison of the results have shown some possibilities and limitations of the tools. Furthermore, aspects of the handling, partly subjective, have emerged when working with the tools. In order to be able to classify the findings, it was qualitatively compared with CFD for which computational costs, fidelity, etc. were assumed to be very high. The properties of the tools were then ranked and evaluated according to this.

4.3.1. DUST

The calculations of the Caradonna-Tung rotor performed in *DUST* were consistently very robust. This observation was to be expected based on the simulations performed by A^3 in collaboration with Politecnico di Milano [42]. Thus, by modeling the wake with vortex particles, robust calculations can be carried out especially in simulations with aerodynamic interactions between bodies and the wake [42].

The initial preparation of a simulation usually involves effort if no prior knowledge is available and the simulation itself is also time-consuming. The required characteristic values, such as C_T and C_Q , must be calculated independently from the total forces or total moments and the force distributions. This must be done after the simulation, and therefore some time is also required for post-processing if automation has not yet been implemented. If one decides to use LL instead of VLM or SP for modeling the lifting surfaces, the C_l , C_d and C_m distributions can be determined, but these characteristic values are only determined using look-up tables.

Basic features:

- Reliable and robust simulation due to vortex particle wake
- Different fidelity levels (LL, VLM, SP)
- Aeroacoustic analyses possible

Restrictions:

- Parametric creation of geometry time-consuming
- Modelling, calculation and post-processing only via scripts
- Does not consider stalls [20]

Future:

- Capture of stalls [20]

The functions that take stalls into account are already in preparation. However, the computation time is not intended to suffer and remain an order of magnitude below CFD simulations [20].

4.3.2. FLOWLab

Since the VPM solver is not publicly available, many of the advantages of the *FLOWUnsteady* tool developed by *FLOWLab* cannot be used. Instead, the quasi-steady solver, which uses VLM, can be used, which captures wing-rotor interactions. However, according to *FLOWLab* [28], rotor-rotor interactions are only minimally captured. This weakness has also been noticeable in the simulation of the Vahana configuration. By using the quasi-steady solver instead of the VPM solver, however, less computing power is required and simulations are carried out comparatively quickly. Simulation preparation, on the other hand, is time-consuming, unless pre-built scripts are used and adapted to the current application for pre- and post-processing. In addition to a condition in which the inflow conditions, rotor speeds, rotor pitch angles, tilt angles, etc. are kept constant, a kinematic maneuver can be specified over a given trajectory with variable parameters. For example, the analysis of an eVTOL configuration can be carried out from the take-off process, through the transition, the cruise flight, to the landing process. For each point in time, desired parameters of the entire system but also of individual components, such as certain rotors, can be obtained.

Basic features:

- Fast simulation with the quasi-steady solver
- Analysis of a configuration along a defined kinematic manoeuvre
- Aeroacoustic analyses
- Embedding in Julia programs for optimisation possible

Restrictions:

- With open source tools only quasi-steady simulations possible
- No friction drag is captured via VLM

Future [43]:

- VPM open source
- Coupling of aerodynamic forces and the trajectory to enable dynamic simulations
- Flow separation at blunt bodies and friction drag

4.3.3. SARF

SARF enables fast pre-processing, fast simulation execution and post-processing with comparably low effort and while still delivering acceptable results. Especially the geometry creation via a GUI and the use of the rotor database can save time already during the simulation preparation. The implemented DLM solver performs the simulation comparatively quickly and good results are achieved by representing transient effects. The results can be obtained immediately through the automatic calculation of important parameters and through the automatic visualization. The limit on the number of concurrently simulated objects and missing consideration of friction drag is currently hindering the effective application of the tool for configurations, that go beyond a rotor/wing combination. Furthermore, it is also currently not possible to predict or enforce stall and flow separation effects.

Basic features:

- The creation of geometry is facilitated by a GUI
- Blocking effects not included in the VLM are captured and represented by additional terms
- Fast and easy model generation
- Large number of automatically calculated parameters
- Kinematic manoeuvres
- Growing database with common rotors

Restrictions:

- Currently, only one rotor/wing combination can be analyzed at a time
- No thickness effects are represented in the current model, therefore only induced drag (and induced torque) is calculated.
- Wing/rotor stall is not captured
- Not open source

Future:

- Representation of friction drag
- Representation of stall behavior
- Simulation of more complex configurations

4.3.4. OpenVSP/VSPAero

OpenVSP models are configured via a graphical user interface through which components are created and adjusted by parameter settings. A 3-dimensional representation of the geometry provides direct feedback on the settings made. The integrated analysis tool *VSPAero* then enables simple and fast pre-processing and the actual computation. The quality of the results has been shown to potentially differ greatly from results of other tools. The result manager and viewer implemented in *VSPAero* enable a fast evaluation of the results.

Basic features:

- *OpenVSP* user interface for geometry creation
- *VSPAero* user interface for simulation settings
- All relevant aerodynamic parameters available in one „Result-Manager“.
- Database of configurations

TAB 2. Overview of the compared tools for aerodynamic rotor analyses

Tool	Wake solver	Modelling effort	Computational cost	Post-processing effort	Fidelity	Transient effects
<i>DUST</i>	VPM	medium	medium	high	medium/high	✓
<i>FLOWLab</i> ¹	VLM	medium	medium	medium	medium	quasi-steady
<i>SARF</i>	DLM	low/medium	low	low	medium	✓
<i>VSPAero</i>	VLM	low	low	low	low	✗
<i>CFD</i>	-	very high	very high	very high	very high	✓

Restrictions:

- Unstable rotor wake at low speeds and rotor pitch angles
- Only VLM applicable, panel method is hardly executable
- Only simplified VSP models can be used

4.4. Final Comparison

By comparing the results of the benchmark case and the VTOL transition case, advantages and disadvantages of the tools were derived. It was observed that certain advantages of the methods used for wake modeling cannot necessarily be exploited due to the special features of the tools. Above all, preparation and post-processing play an important role here. Table 2 gives an overview of important aspects of the rotor aerodynamics tools.

In order to be able to classify the findings, it was qualitatively compared with CFD for which computational costs, fidelity, etc. were assumed to be very high. The properties of the tools were then ranked according to this.

As mentioned, the classification shown here applies to the first implementation, where the scripts for pre- and post-processing as well as the calculations must be created or sample scripts from the creators are adapted.

If the goal is to perform a quick evaluation with acceptable results, *VSPAero* can be used. The intuitive parametric generation of the geometry via the user interface brings many advantages. The geometry can be adjusted arbitrarily and iteratively while changes are immediately displayed graphically. The large number of calculated output parameters and the integrated visualization allow for a fast evaluation. However, frequently occurring instabilities can cause major problems when using *VSPAero*.

If it is intended to only evaluate a single rotor/wing combination, *SARF* is particularly suitable. A model can be generated relatively quickly via a GUI or by accessing a rotor or wing from the database. The DLM solver used in the calculation represents the transient effects of the wake quite well. Good results can be obtained with a short calculation time, which are automatically visualized. Furthermore, the automatic calculation of important parameters can save a lot of time in post-processing. However, *SARF* is not yet open source and is currently not able to estimate the friction drag on any object.

¹without VPM-Solver, using quasi-steady solver

Results at a high level can be obtained with *DUST*. For complex configurations, it is advantageous to have a CGNS model available, as the modeling effort via parametric creation would otherwise be high. The visualization of the results, on the other hand, requires little effort. The transient effects of the wake over the particles can be visualized well due to the VPM. The calculation of the parameters has to be carried out mainly by the user, at least for the first execution of the simulation.

FLOWLab's publicly available quasi-steady solver gives acceptable results. Much more promising is the VPM that can be used in the future. According to Alvarez and Ning [27] the VPM should provide high-quality results for complex multi-rotor configurations. The effort for the model generation can vary greatly. Time can be saved by using and adapting existing *FLOWLab* scripts. For rotors and lifting surfaces, an automatic calculation of the characteristic values and an automatic visualization can be carried out.

5. SUMMARY AND CONCLUSION

The work gives an overview of selected rotor aerodynamics tools and compares them. The analyzed tools are *DUST*, developed by Airbus A³ and the Politecnico di Milano, the tool packages from the *BYU FLOWLab*, *SARF* from TU Munich and *OpenVSP/VSPAero*.

5.1. Summary

Two cases, the Caradonna-Tung rotor and the Airbus A³ Vahana, are used for the comparison. The Caradonna-Tung rotor is used because of the available experimental data and serves as a benchmark case. The Airbus A³ Vahana tilt-wing system represents a real-world eVTOL configuration with complex aerodynamic effects, for which the properties of a main wing rotor are investigated in different flight phases. The results are compared by means of the thrust coefficient, the torque coefficient, the local lift coefficient, the Figure of Merit and the efficiency. Overall compatibility in terms of geometric and numerical discretization is a crucial aspect and ensured for all cases and tools.

The results show, that all tools can simulate both cases successfully by means of convergence. In the benchmark case, the results were validated with experimental data, compared across all tools and deviations were discussed. For the validation of the tools, the distribution of the

lift coefficient C_l was used. Good agreement with the experimental results was shown. The cross-method comparison was carried out on the basis of the parameters C_T , C_Q and FOM obtained with varying rotor speed Ω_{Rotor} and varying rotor pitch angle Θ_C . For $\Theta_C = 5^\circ$ deviations of less than 30% could be found. The increasingly transient wake at larger pitch angles Θ_C could only be reproduced by *SARF* and *DUST*. The A³ Vahana was also modeled in three tools, simulated and compared across methods. For the implementation of the Vahana in *DUST*, a paper by A³ and the Politecnico di Milano was consulted and relevant parameters for the climb, the mid-transition and the late-transition were derived. When comparing the VTOL transition case between the tools C_T , C_Q and η were considered. The deviations caused by the different numerical approaches were identified and discussed. The comparison showed major differences in the modelling and approach of the calculation methodology so that many aspects of the tools could not be directly compared quantitatively. Specifics and limitations were derived from the benchmark case and the VTOL transition case. Guidelines and recommendations for tool selection were elaborated, which make it possible to choose the most suitable tool for modelling for a given use case. In addition, aspects of handling and ease of use were described.

The innovations and improvements of the tools under consideration should be taken into account. The most promising tools will be used in future work to simulate the flight mechanics needed for the development of eVTOL control architectures.

5.2. Conclusion

This paper provides an overview of promising tools for rotor aerodynamics and rotor blade analysis. The possibilities offered by individual tools are shown, but limitations are also pointed out. The aspects to be considered with regard to handling and use are also discussed. It has been shown that the tools can provide accurate results with relatively little computational effort if the computational parameters are chosen carefully. For further applications, this work serves as a decision-making aid through which a choice of a rotor aerodynamics tool can be made depending on the desired accuracy, robustness, user interface etc.

Contact address:

daniel.perdolt@tum.de

6. REFERENCES

- [1] Raoul Rothfeld, Anna Straubinger, Mengying Fu, Christelle Al Haddad, and Constantinos Antoniou. Urban air mobility. In *Demand for Emerging Transportation Systems*, pages 267–284. Elsevier, 2020. DOI: [10.1016/B978-0-12-815018-4.00013-9](https://doi.org/10.1016/B978-0-12-815018-4.00013-9).
- [2] Satadru Roy, Apoorv Maheshwari, William A. Crossley, and Daniel A. DeLaurentis. Future Regional Air Mobility Analysis Using Conventional, Electric, and Autonomous Vehicles. *Journal of Air Transportation*, 29(3):113–126, 2021. DOI: [10.2514/1.D0235](https://doi.org/10.2514/1.D0235).
- [3] Mengying Fu, Raoul Rothfeld, and Constantinos Antoniou. Exploring Preferences for Transportation Modes in an Urban Air Mobility Environment: Munich Case Study. *Transportation Research Record: Journal of the Transportation Research Board*, 2673(10):427–442, 2019. DOI: [10.1177/0361198119843858](https://doi.org/10.1177/0361198119843858).
- [4] Matthew Daskilewicz, Brian German, Matthew Warren, Laurie A. Garrow, Sreekar-Shashank Boddupalli, and Thomas H. Douthat. Progress in Vertiport Placement and Estimating Aircraft Range Requirements for eVTOL Daily Commuting. In *2018 Aviation Technology*. DOI: [10.2514/6.2018-2884](https://doi.org/10.2514/6.2018-2884).
- [5] Shamsheer S. Chauhan and Joaquim R. R. A. Martins. Tilt-Wing eVTOL Takeoff Trajectory Optimization. *Journal of Aircraft*, 57(1):93–112, 2020. DOI: [10.2514/1.C035476](https://doi.org/10.2514/1.C035476).
- [6] Alessandro Bacchini. *Electric VTOL preliminary design and wind tunnel tests*. PhD thesis, Politecnico di Torino, 29.02.2020.
- [7] Felix Finger, Carsten Braun, and Cees Bil. A review of configuration design for distributed propulsion transitioning vtol aircraft. In *Asia-Pacific International Symposium on Aerospace Technology 2017, APISAT 2017, Seoul, Korea*, 2018.
- [8] Tom C. A. Stokkermans, Daniele Usai, Tomas Sinnige, and Leo L. M. Veldhuis. Aerodynamic Interaction Effects Between Propellers in Typical eVTOL Vehicle Configurations. *Journal of Aircraft*, 58(4):815–833, 2021. DOI: [10.2514/1.C035814](https://doi.org/10.2514/1.C035814).
- [9] Dhwanil Shukla and Narayanan Komerath. Multirotor Drone Aerodynamic Interaction Investigation. *Drones*, 2(4):43, 2018. DOI: [10.3390/drones2040043](https://doi.org/10.3390/drones2040043).
- [10] Patrick C. Murphy, David Hatke, Vanessa V. Aubuchon, Rose Weinstein, and Ronald C. Busan. Preliminary Steps in Developing Rapid Aero Modeling Technology. In *AIAA Scitech 2020 Forum*, Reston, Virginia, 01062020. American Institute of Aeronautics and Astronautics. DOI: [10.2514/6.2020-0764](https://doi.org/10.2514/6.2020-0764).
- [11] Benjamin M. Simmons and Patrick C. Murphy. Wind Tunnel-Based Aerodynamic Model Identification for a Tilt-Wing, Distributed Electric Propulsion Aircraft. In *AIAA Scitech 2021 Forum*, Reston, Virginia, 01112021. American Institute of Aeronautics and Astronautics. DOI: [10.2514/6.2021-1298](https://doi.org/10.2514/6.2021-1298).
- [12] Benjamin M. Simmons, Pieter G. Buning, and Patrick C. Murphy. Full-Envelope Aero-Propulsive Model Identification for Lift+Cruise Aircraft Using Computational Experiments. In *AIAA AVIATION 2021 FORUM*, Reston, Virginia, 08022021. American Institute of Aeronautics and Astronautics. DOI: [10.2514/6.2021-3170](https://doi.org/10.2514/6.2021-3170).
- [13] Alex Zanotti, Alberto Savino, Michele Palazzi, Matteo Tugnoli, and Vincenzo Muscarello. Assessment of a Mid-Fidelity Numerical Approach for the Investigation of Tiltrotor Aerodynamics. *Applied Sciences*, 11(8):3385, 2021. DOI: [10.3390/app11083385](https://doi.org/10.3390/app11083385).
- [14] F. X. Caradonna and C. Tung. Experimental and Analytical Studies of a Model Helicopter Rotor in Hover, 1981.
- [15] Benjamin Simmons, Pieter Buning, and Patrick Murphy. Full-envelope aero-propulsive model identification for lift+cruise aircraft using computational exper-

- iments. In *AIAA AVIATION 2021 Forum*, 08 2021. DOI: [10.2514/6.2021-3170](https://doi.org/10.2514/6.2021-3170).
- [16] Wayne Johnson. Ndac-nasa design and analysis of rotorcraft. Technical report, NASA, 2015.
- [17] R. Healy, Matthew Misiorowski, and F. Gandhi. A systematic cfd-based examination of rotor-rotor separation effects on interactional aerodynamics for large evtol aircraft. In *Proceedings of the 75th Vertical Flight Society Annual Forum*, 2019.
- [18] Zhongqi Jia and Seongkyu Lee. Acoustic analysis of a quadrotor evtol design via high-fidelity simulations. In *25th AIAA/CEAS Aeroacoustics Conference*, 2019. DOI: [10.2514/6.2019-2631](https://doi.org/10.2514/6.2019-2631).
- [19] Jacob Cook. A strip theory approach to dynamic modeling of evtol aircraft. In *AIAA Scitech 2021 Forum*, 2021. DOI: [10.2514/6.2021-1720](https://doi.org/10.2514/6.2021-1720).
- [20] Davide Montagnani, Matteo Tugnoli, Alex Zanotti, Monica Syal, and Giovanni Droandi. Analysis of the Interactional Aerodynamics of the Vahana eVTOL Using a Medium Fidelity Open Source Tool. In *Proceedings of the VFS Aeromechanics for Advanced Vertical Flight-Technical Meeting*, 2020.
- [21] Davide Montagnani, Matteo Tugnoli, Federico Fonte, and Alex Zanotti, editors. *Mid-Fidelity Analysis of Unsteady Interactional Aerodynamics of Complex VTOL Configurations*, 2019.
- [22] Gregoire Stephane Winckelmans. *Topics in vortex methods for the computation of three- and two-dimensional incompressible unsteady flows*. PhD thesis, California Institute of Technology, 1989. DOI: [10.7907/19HD-DF80](https://doi.org/10.7907/19HD-DF80).
- [23] Georges-Henri Cottet and Petros D. Koumoutsakos. *Vortex methods: Theory and practice*. Cambridge Univ. Press, Cambridge, 2000. ISBN: 9780521621861. DOI: [10.1017/CBO9780511526442](https://doi.org/10.1017/CBO9780511526442).
- [24] FLOWUnsteady. <https://flow.byu.edu/FLOWUnsteady/>, 09.07.2021.
- [25] Eduardo J. Alvarez and Andrew Ning, editors. *Development of a Vortex Particle Code for the Modeling of Wake Interaction in Distributed Propulsion*, 2018. DOI: [10.2514/6.2018-3646](https://doi.org/10.2514/6.2018-3646).
- [26] Eduardo Alvarez and Andrew Ning, editors. *Modeling Multirotor Aerodynamic Interactions Through the Vortex Particle Method*, 2019. DOI: [10.2514/6.2019-2827](https://doi.org/10.2514/6.2019-2827).
- [27] Eduardo J. Alvarez and Andrew Ning. High-Fidelity Modeling of Multirotor Aerodynamic Interactions for Aircraft Design. *AIAA Journal*, 58(10):4385–4400, 2020. DOI: [10.2514/1.J059178](https://doi.org/10.2514/1.J059178).
- [28] Eduardo J. Alvarez. Quasi-steady Aerodynamics Solver for a High-fidelity Controls Framework, 2020.
- [29] Eduardo J. Alvarez and Andrew Ning. Unsteady Mixed-fidelity Aerodynamics Solver for Maneuvering Multirotor Aircraft, 2021.
- [30] Moritz Thiele. Erweiterung und Validierung eines Rotor-tools mit Konfigurationsstudie, 2016.
- [31] Moritz Thiele, Dimitrios Salassidis, and Mirko Hornung. Propeller Wake - Object Interaction using a Free Wake Model utilizing Local Mesh Separation. 2021.
- [32] Nasa. OpenVSP, 09.07.2021.
- [33] Daniel Böhnke, Björn Nagel, Mengmeng Zhang, and Arthur Rizzi, editors. *Towards a Collaborative and Integrated Set of Open Tools for Aircraft Design*, Reston, Virginia, 2013. American Institute of Aeronautics and Astronautics. DOI: [10.2514/MASM13](https://doi.org/10.2514/MASM13).
- [34] OpenVSP. Learn More About OpenVSP, 09.07.2021.
- [35] Richard Harrison. Using VSPAero to generate an aerodynamic model for JSBSim in FlightGear: Richard Harrison’s development notes, 09.07.2021.
- [36] Robert Alan McDonald, editor. *Advanced Modeling in OpenVSP*, Reston, Virginia, 06132016. American Institute of Aeronautics and Astronautics. DOI: [10.2514/MATIO16](https://doi.org/10.2514/MATIO16).
- [37] Jason Fugate, Nhan Nguyen, and Juntao Xiong, editors. *Aero-Structural Modeling of the Truss-Braced Wing Aircraft Using Potential Method with Correction Methods for Transonic Viscous Flow and Wing-Strut Interference Aerodynamics*, Reston, Virginia, 06172019. American Institute of Aeronautics and Astronautics. DOI: [10.2514/MAVIAT19](https://doi.org/10.2514/MAVIAT19).
- [38] J. Gordon Leishman. *Principles of helicopter aerodynamics*. Cambridge aerospace series. Cambridge University Press, Cambridge, United Kingdom, second edition edition, 2017. ISBN: 9781107013353.
- [39] Acubed. Certifying AI for Safety Critical Aircraft Systems, 01.08.2021.
- [40] BYU FLOW Lab. : <https://github.com/byuflowlab/FLOWUnsteady/>, 24.08.2021.
- [41] Chengjian He and Jinggen Zhao. Modeling Rotor Wake Dynamics with Viscous Vortex Particle Method. *AIAA Journal*, 47(4):902–915, 2009. DOI: [10.2514/1.36466](https://doi.org/10.2514/1.36466).
- [42] Monica Syal, Davide Montagnani, Matteo Tugnoli, Alex Zanotti, and Giovanni Droandi. Analysis of the Interactional Aerodynamics of the Vahana eVTOL Using a Medium Fidelity Open Source Tool, 2020.
- [43] Eduardo J. Alvarez. FLOW Lab , BYU: <https://flow.byu.edu/>, 12.08.2021.